EEET ECOLOGICAL ENGINEERING & ENVIRONMENTAL TECHNOLOGY

Ecological Engineering & Environmental Technology, 2026, 27(5), 270–279
https://doi.org/10.12912/27197050/220314
ISSN 2719–7050, License CC-BY 4.0

Received: 2026.03.17
Accepted: 2026.04.15
Published: 2026.05.01

Anatomical markers of interclonal needle variability in Scots pine seedlings at early ontogenetic stages

Taras Vaskiv[1], Artur Likhanov[1], Volodymyr Gryb[1], Hanna Mazurchuk[1], Nataliia Puzrina[1], Roman Vasylyshyn[1], Oleksandr Bala[1], Yevhenii Khan[1], Anatolii Karpuk[2], Oleksandr Melnyk[2]

[1] Education and Research Institute of Forestry and Landscape-Park Management, National University of Life and Environmental Sciences of Ukraine, Heroiv Oborony Str., 15, Kyiv, Ukraine
[2] NUBiP of Ukraine Boyarka Forest Research Station, 08150, Lisodoslydna Str., 12, Boyarka, Ukraine
* Corresponding author's e-mail: bala@nubip.edu.ua

ABSTRACT

The study aimed to determine needle morphometric traits in seedlings of different clonal origin and to assess their variability. The anatomical structure of needles may reflect the functional status of Scots pine (*Pinus sylvestris* L.) seedlings at early ontogenetic stages. Seedlings of three clones – D1 (slow-growing) and D21, D22 (fast-growing) – were examined using light and fluorescence microscopy with digital image analysis (Image-Pro Premier 10.0). Statistical analyses included one-way ANOVA with Tukey's HSD post hoc test, principal component analysis (PCA), and partial least squares discriminant analysis (PLS-DA). Analysis of needle anatomical parameters in Scots pine seedlings confirms that fast growth (clones D21 and D22) is associated with certain anatomical features compared to the slow-growing clone D1. Fast-growing clones typically have a more developed vascular system (wider phloem and xylem) and better structural protection (thicker cuticle and resin duct sclerenchyma). However, the variability in certain parameters – notably plicate mesophyll thickness and resin duct diameter – suggests that fast growth may result from different combinations of anatomical characteristics and compensatory mechanisms. Fluorescence microscopy data confirmed higher tissue autofluorescence intensity in clones D21 and D22 compared to the slow-growing clone, suggesting differences in cell wall composition and structure, as well as in the content of fluorescently active cellular components. Multivariate analysis (PCA and PLS-DA) revealed clear clustering of the studied clones and identified plicate mesophyll width, phloem width, and resin duct diameter as the anatomical traits contributing most to interclonal differentiation. The identified morpho-anatomical traits can serve as early-stage selection criteria for Scots pine seedlings, potentially reducing dependence on prolonged field trials. This is the first quantitative characterisation of the needle morpho-anatomical trait complex in Scots pine clonal seedlings at early developmental stages.

Keywords: *Pinus sylvestris*, needle anatomy, interclonal variability, morphometric analysis, resin ducts, fluorescence microscopy.

INTRODUCTION

Scots pine (*Pinus sylvestris* L.) is one of the dominant forest-forming tree species of the temperate zone, widely used in forestry for the restoration and conservation of forest ecosystems (Hordienko et al., 2005; Fuchylo et al., 2021). The species demonstrates high vitality and regeneration capacity across the Polissia forest-steppe, and steppe zones of Ukraine (Humeniuk, 2015; Lovynska et al., 2021).

Under ongoing climate change, there is a growing need to select plants with enhanced resilience to abiotic and biotic stresses driven by shifts in temperature regimes, water balance, and increasing frequency of extreme weather events (IPCC, 2021; Allen et al., 2015). Traditional approaches to assessing the adaptive traits of woody

plants rely on long-term field observations, which considerably hamper early selection of promising genotypes and prolong the breeding cycle (Babyn et al., 2024b).

At the same time, for Scots pine and most conifer species, assessing resilience and phenotypic plasticity of planting stock at early ontogenetic stages is particularly important, as the initial developmental phases are most sensitive to water deficit and temperature stress (Reich and Oleksyn, 2008; Savill, 1991), and to infection by phytopathogenic fungi of various taxonomic groups (Boyko and Puzrina, 2021). Therefore, identifying morpho-anatomical traits that allow identification of seedlings with enhanced adaptive capacity to changing environmental conditions is of particular relevance (Boyko et al., 2021; Pinchuk et al., 2020; Pinchuk et al., 2021).

Current research indicates that needle microstructure is among the most responsive systems, being the first to react to changes in environmental conditions (Oberhuber et al., 2015). Needle anatomical elements – cuticle, epidermis, hypodermis, mesophyll, vascular tissues, and resin ducts – reflect the degree of structural differentiation of the assimilatory apparatus and can serve as markers of plant functional status (Evert, 2006; Vaganov et al., 2006).

Needle anatomical traits such as cell wall thickness, degree of epidermis development, presence of hypodermis, and vascular bundle architecture are regarded as indicators of seedling physiological status and are associated with resilience to water deficit, frost, or overheating. In *Pinus sylvestris* L., morpho-anatomical needle traits, including vascular element characteristics, vary along climatic gradients and are interpreted as adaptive responses to adverse environmental conditions (Reich and Oleksyn, 2008).

Available evidence suggests that needle anatomical traits reflect the physiological status and adaptive potential of seedlings (Oberhuber et al., (2015). However, to date, no systematic quantitative study has compared needle anatomical traits across Scots pine clones at the seedling stage or evaluated their potential as early markers of clone-level adaptive differentiation. This knowledge gap is particularly significant given the growing need to accelerate genotype selection under climate change conditions. Therefore, this study aims to characterise the anatomical structure of needles in Scots pine (*Pinus sylvestris* L.) seedlings of different clonal origin at early developmental stages, and to identify morpho-anatomical traits associated with seedling growth potential and adaptive capacity. The following hypotheses were tested: 1 – needle anatomical traits differ significantly among Scots pine clones at early ontogenetic stages; 2 – clones with more developed epidermal and hypodermal layers demonstrate higher potential resilience to abiotic stresses (water deficit, temperature fluctuations); 3 – needle anatomical traits, specifically vascular bundle characteristics and mesophyll structure, correlate with early growth vigour and biometric performance in seedlings.

MATERIALS AND METHODS

Sixty clones of Scots pine (*Pinus sylvestris* L.) were selected from superior stands and gene conservation areas in the Polissia zone of Ukraine (coordinates: 50.704264°N, 29.694646°E). Selection criteria included above-average growth rate, seed production, and health status assessed during 2023. Each clone was assigned a code (D1–D60) for identification in tables, figures, and statistical analyses.

During the first large-scale collection in 2016–2017, 10,917 kg of cones were collected, yielding 168 kg of seeds with an average yield of 1.54%. Control seedlings were grown from local seeds collected in accordance with standard operating procedures from elite trees, without regard to clonal identity. In April 2023, experimental plots were established for the germination of genetically improved Scots pine (*Pinus sylvestris* L.) seeds in open ground. Seeds were collected and dried separately for each clone to enable subsequent tracing of seedlings by clonal origin. Prior to sowing, the seeds were soaked for 16 hours (2 May 2023). On 3 May 2023, 12 g of seeds were sown on each marked plot in accordance with the experimental design, corresponding to 1.500 seeds per 1 m². The sowing rate was 120 seeds per linear metre of the seed furrow. The size of a single plot was 0.5 × 2.0 m. Germination was recorded on 19 May 2023.

The soil medium under controlled conditions consisted of bark and peat in a ratio of 7:3. The topsoil was loosened, levelled, and covered with a 2 cm layer of white sand.. The seeds were distributed evenly, covered with sifted sand, pressed into the medium using a roller, and shaded. Watering was carried out in the evening when the

daytime heat had subsided; the frequency of watering was adjusted depending on soil moisture to avoid drying out or waterlogging. During the growing season, 3–4 foliar feedings were carried out in accordance with phenological observations.

The experimental material of seedlings was grown in trays. Monitoring of germinated seedlings was conducted during September-October 2024 by recording biometric parameters: height, root collar diameter, needle length, root length (taproot and lateral roots), and total seedling count**.** For needle anatomical analysis, seedlings were selected based on their biometric parameters.

Among the 60 clones studied, clones with the lowest and highest biometric values were identified: clone D1 (slow-growing) and clones D21 and D22 (fast-growing). Ten seedlings were sampled per clone, and five needles were collected from each seedling for anatomical analysis. Needles were harvested from the mid-portion of the current-year shoot increment (n = 10 per clone). Transverse sections approximately 50–100 μm thick were prepared manually using a scalpel under a stereomicroscope. Three to five sections were taken from each needle; these were mounted on glycerol-coated slides and examined using an inverted fluorescence microscope. Microscopic examinations were carried out in 2024 at the Biotechnology and Cell Engineering Laboratory, National University of Life and Environmental Sciences of Ukraine.

Needle samples were incubated for 6 hours in a stabilizing solution of glycerin : ethanol : water (v/v/v 1:1:1) to preserve tissue integrity. Transverse needle sections were prepared manually using a precision scalpel. To ensure reproducibility and minimize error in the quantitative autofluorescence analysis, a selective sampling approach was employed. Only sections with a thickness of 35 ± 5 μm were selected for further investigation. Section thickness was verified immediately after cutting (prior to mounting) using a digital micrometer with a resolution of 0.001 mm. Measurements were performed with minimal contact force to prevent deformation of the soft needle tissues. The prepared sections were mounted on glass slides in distilled water.

Needle tissue anatomy was examined using an inverted microscope equipped with a multichannel fluorescence imaging system (EVOS FL System, Thermo Fisher Scientific, USA) employing three filter channels: DAPI (357/44 nm), GFP (482/25 nm), and Texas Red (585/29 nm).

Autofluorescence intensity was used to assess overall tissue metabolic activity and the content of chlorophylls, lignin, flavonoids, and other phenolic compounds.

Morphometric measurements were performed using Image-Pro Premier 10.0 software (Media Cybernetics, USA). Statistical processing was performed using SigmaPlot 13.0 (Supplementary Materials 2). Data normality and homogeneity of variance were assessed using Shapiro-Wilk and Equal Variance tests, respectively. One-Way ANOVA followed by the Tukey post-hoc test was applied. For data with non-normal distribution or unequal variances, the Kruskal-Wallis ANOVA on Ranks with the Tukey test was used. The significance level was set at $p < 0.05$. Detailed statistical reports are provided in the Supplementary Materials. Multivariate statistical analysis, including principal component analysis (PCA), partial least squares discriminant analysis (PLS-DA), was performed using the MetaboAnalyst 6.0 online platform. Multivariate analyses were performed, including principal component analysis (PCA), partial least squares discriminant analysis (PLS-DA), and hierarchical cluster analysis.

RESULTS

Given the contrasting biometric characteristics observed, three representative clones were selected from the total of 60 studied clones for subsequent anatomical and fluorescence analysis: D1 (slow-growing) and D21 and D22 (fast-growing). The control group consisted of seedlings grown from Scots pine seed of local provenance. One-way analysis of variance (ANOVA, $p < 0.05$) revealed statistically significant differences among clones in needle length of Scots pine seedlings (Figure 1).

The analysis included n = 10 seedlings per variant. The lowest mean needle length was recorded for clone D1 at 1.2 ± 0.2 cm, while the highest values were observed in clones D21 and D22 at 4.4 ± 0.1 cm, substantially exceeding the control (3.2 ± 0.1 cm). Low standard error values indicate the relative stability of this parameter within each variant.

To determine whether the observed contrasts in biometric parameters are accompanied by corresponding changes in needle internal organization, and to assess the presence of anatomical differences among clones with minimum and

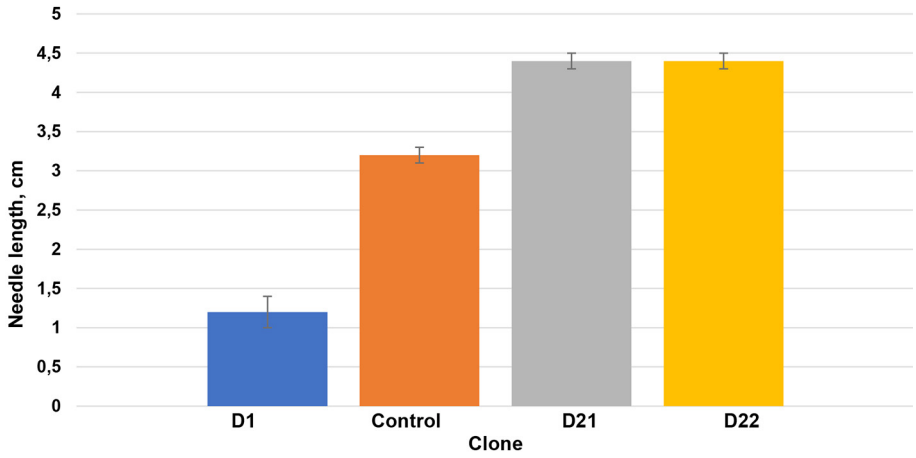

Figure 1. Mean needle length of Scots pine seedlings across clones with standard error bars.
Note: The statistical significance of differences was assessed using one-way analysis of variance (ANOVA, $p < 0.05$) with Tukey's post hoc test. The control group is shown separately

maximum values, needle anatomical analysis was conducted on Scots pine seedlings of different clonal origin.

Anatomical analysis of needles from Scots pine seedlings derived from seeds of different clonal origins revealed statistically significant variability in several morphometric parameters.

Particularly notable were the results for resin duct diameter, which ranged from 22.7 to 41.5 µm. In seedlings with superior biometric parameters (height, root collar diameter), these structures were considerably better developed. Resin ducts are known to perform an important barrier function, participating in chemical defense mechanisms against phytophagous insects and pathogens (Bracalini et al., 2024). The data suggest a possible link between the degree of development of needle anatomical structures and breeding-relevant traits of Scots pine seedlings.

Examination of needle cross-sections under the green channel revealed bright fluorescence of the cuticle overlying epidermal cells, the cell walls of the epidermis, endodermis, and transfusion parenchyma, and the tracheids of the vascular bundle (Figure 2).

Fluorescence microscopy enabled label-free visualization of the internal needle structure of Scots pine seedlings, exploiting the autofluorescence properties of cellular components. Across all experimental variants, intense fluorescence of the cuticle, mechanical tissues, resin ducts, and mesophyll was recorded, with emission brightness varying according to seedling clonal origin. The highest signal intensity in the GFP and Texas Red ranges was observed in seedlings of the variant with superior growth performance, possibly indicating a higher concentration of phenolic compounds and greater structural density of cell walls. According to the literature, the autofluorescence intensity of chloroplasts, lignin, and resinous inclusions is directly related to the degree of tissue maturity and functional status, particularly under abiotic stress conditions (Tereshchenko et al., 2020). The results confirm that fluorescence microscopy is a promising approach for identifying anatomical markers of seedling adaptive resilience to adverse environmental conditions (Babyn et al., 2024a; Derii et al., 2024).

Cuticle thickness in different clones ranged from 1.6 µm (clone D1) to 1.8 µm (clone D22). Epidermal cells of clones D1 and D21 exhibited thickened outer tangential walls, whereas in clone D22, the inner tangential walls were also thickened, suggesting a clone-specific growth pattern driven by high metabolic activity that supports simultaneous formation of both outer and inner cell walls. A characteristic feature of the needles was stomatal formation with guard cells bearing prominently thickened tangential walls. In clone D22, stomata were sunken into the already-developed hypodermis, which was absent in clones D1 and D21 (Table 1, Supplementary Materials 1).

Endodermis width showed a clear trend of increase with growth intensity: the slow-growing clone D1 had the smallest value (34.4 µm), while fast-growing clones D21 (36.5 µm) and D22 (40.0 µm) had progressively greater widths, which may indicate a more developed substance transport system in fast-growing clones. Plicate mesophyll thickness in the slow-growing clone D1 was

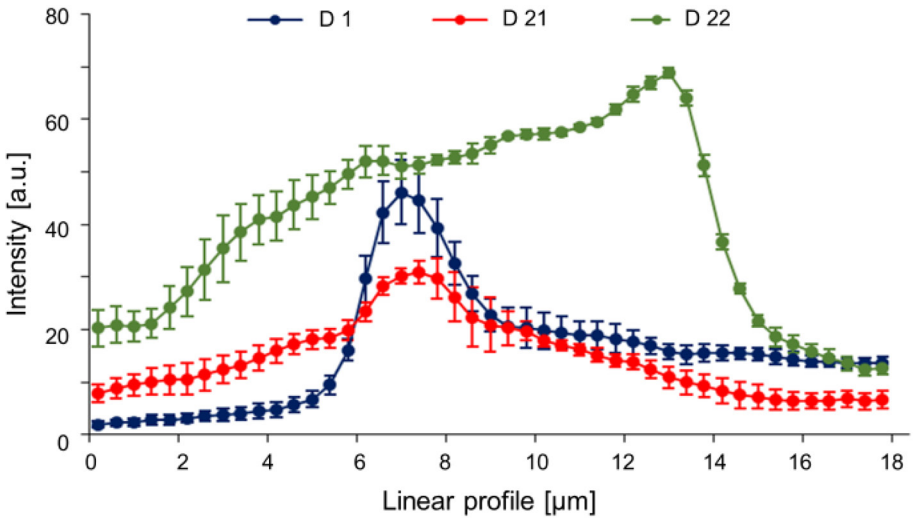

Figure 2. Fluorescence intensity profiles of Scots pine needle epidermal cells in the green spectrum (λ_{exc} = 482/25 nm; λ_{em} = 524/24 nm)

Table 1. Anatomical parameters of Scots pine seedling needles, m ± SE (n = 10)

Parameters, µm	Clone D1	Clone D21	Clone D22
ED height*	24.5 ± 1.16	22.2 ± 1.21	24.7 ± 1.59
ED width	34.4 ± 1.76	36.5 ± 1.37	40.0 ± 1.95
PM thickness	92.7 ± 1.69	116.0 ± 3.61**	65.8 ± 2.57**
Ep height	17.5 ± 0.86	16.8 ± 0.64	10.1 ± 0.41**
Ct thickness	1.6 ± 0.05	1.7 ± 0.06	1.8 ± 0.19
Hp height	0	0	12.1 ± 0.58**
Xy width	31.0 ± 0.91	25.9 ± 0.98**	33.2 ± 1.11
Ph width	26.6 ± 0.69	33.5 ± 0.57*	35.3 ± 1.35*
Xy/Ph	1.2 ± 0.05	0.8 ± 0.02*	0.9 ± 0.04*
RD diameter	32.4 ± 0.59	22.7 ± 0.57**	41.5 ± 1.06**
SRD height	11.6 ± 0.47	16.3 ± 0.45**	17.3 ± 0.53**

Note: * ED – endodermis, PM – plicate mesophyll, Ep – epidermis, Ct – cuticle, Hp – hypodermis, Xy – xylem, Ph – phloem, RD – resin duct, SRD – resin duct sclerenchyma. * – $p < 0.05$; ** – $p < 0.001$ (One–Way ANOVA or Kruskal–Wallis test followed by Tukey post-hoc test).
Detailed statistical reports are provided in the Supplementary Materials 2.

92.7 µm. Fast-growing clones showed considerable variability: D21 had the greatest thickness (116.0 µm), while D22 had the smallest (65.8 µm), suggesting that fast growth may be associated with both increased and decreased thickness of this tissue, depending on other compensatory mechanisms. Cuticle thickness was lowest in the slow-growing clone D1 (1.6 µm) and increased in fast-growing clones (1.7 µm in D21 and 1.8 µm in D22), which may indicate better needle protection in fast-growing clones. Xylem and phloem width are important indicators of water and nutrient transport efficiency. The slow-growing clone D1 had a xylem width of 31.0 µm and a phloem width of 26.6 µm. Fast-growing clones D21 and D22 had greater phloem width (33.5–35.3 µm) compared to D1, and greater xylem width in D22 (33.2 µm), although xylem width in D21 (25.9 µm) was smaller than in D1, confirming that fast growth is generally associated with a more developed vascular system. Resin duct sclerenchyma cell height was smallest in clone D1 (11.6 µm), while fast-growing clones had greater values (16.3 µm in D21 and 17.3 µm in D22), which may indicate a stronger structure and better protection of the resin ducts in fast-growing clones. The wide variation in the thickness of the pine needle mesophyll in the fast-growing clones

D21 and D22, ranging from 65.8 to 116.0 μm is primarily due to adaptive responses to environmental factors, as well as the genetic characteristics of the stands, which is primarily attributable to the genetic characteristics of the clones, which determine the degree of development and chloroplast density of the plicate mesophyll, this is confirmed by research (Tereshchenko et al., 2020).

Prior to analysis, needles were fixed in 70% ethanol and stored at 4 °C for no more than 7 days. Transverse sections of approximately 50–100 μm thickness were prepared manually using a sharp scalpel (Feather S35) under a stereomicroscope (MBS-10). Sections were consistently obtained from the anatomically standardized mid-needle position (50% of needle length measured from the base). Five sections per needle were prepared, and the three morphologically most representative sections were selected for morphometric measurement. Autofluorescence intensity was quantified using Image-Pro Premier 10.0 software as the mean grey value within defined regions of interest, and values were normalized to the cross-sectional area of the respective tissue compartment (μm^2) to enable inter-clone comparison independent of section thickness variation (Figure 3).

Hypodermis formation provides an additional tissue barrier that protects the internal tissues of the assimilatory organ upon epidermis damage. The hypodermis also regulates the rate of cuticular transpiration, particularly during winter, and shields mesophyll cells from low temperatures. Beneath the hypodermis, the green channel faintly revealed the multilayered plicate mesophyll and the cell walls of the sclerenchyma sheath surrounding the schizogenous resin ducts located in the subepidermal cell layer. The plicate mesophyll fluoresced brightly in the red spectrum owing to the high chloroplast content. The sclerenchyma sheaths of the resin ducts fluoresced in the blue spectrum. Intense sclerenchyma fluorescence was observed in clones D1 and D22, whereas in clone D21 it was comparatively weak in the blue spectrum, possibly indicating slower accumulation of phenolic compounds in the cell walls that impart rigidity to the polysaccharide matrix.

Resin ducts displayed a typical rounded outline, lined with thin-walled secretory epithelial cells that synthesize and secrete resinous substances into the duct lumen. In the central part of the needle, relatively large endodermis and transfusion parenchyma cells were prominent in the green and blue spectra.

The results of multivariate analysis of Scots pine needle anatomical traits using PCA and partial least squares discriminant analysis (PLS-DA) are presented in Figure 4.

The PCA score plot (Figure 4a) shows the distribution of needle anatomical traits across clones (D1, D21, and D22) in the space defined by the first two principal components (PC1 and PC2). Each data point represents the set of anatomical traits for an individual needle sample, with color coding indicating clone identity. The PC1 axis accounts for the largest proportion of total variance (64.8%) in the anatomical trait data, while PC2 accounts for the second-largest share (17.9%). The distance between data points on the plot reflects the degree of similarity or dissimilarity among samples based on their anatomical traits.

PCA revealed clear group separation among the studied clones, indicating pronounced interclonal variability in needle anatomy. It is worth noting that needle anatomical traits of clones D21 and D22 differed most along the first principal component, whereas differences along the second principal component were most pronounced among clones D1 and D22. A similar pattern of sample separation based on a combination of needle anatomical parameters has previously been reported by other authors, who demonstrated that it is precisely the combination of assimilatory, vascular, and secretory tissue parameters that drives effective genotype discrimination in Scots pine at the intraspecific level.

Discriminant analysis, aimed at verifying the significance of sample grouping by a set of traits, confirmed statistically significant differences in needle anatomy among seedlings of different clones. Similar results have been obtained in studies where multivariate statistical methods were applied to assess the morpho-anatomical differentiation of conifer needles, demonstrating their high informativeness for detecting genetically determined differences among populations and clones.

The clone separation shown in the plot (Figure 4b) confirms that the needle anatomy of Scots pine seedlings is characterized by considerable intraspecific variability that develops already at early ontogenetic stages, which is consistent with current understanding of the role of anatomical traits as sensitive markers of adaptive potential in coniferous plants.

ANOVA results showed that among the needle anatomical traits, plicate mesophyll width

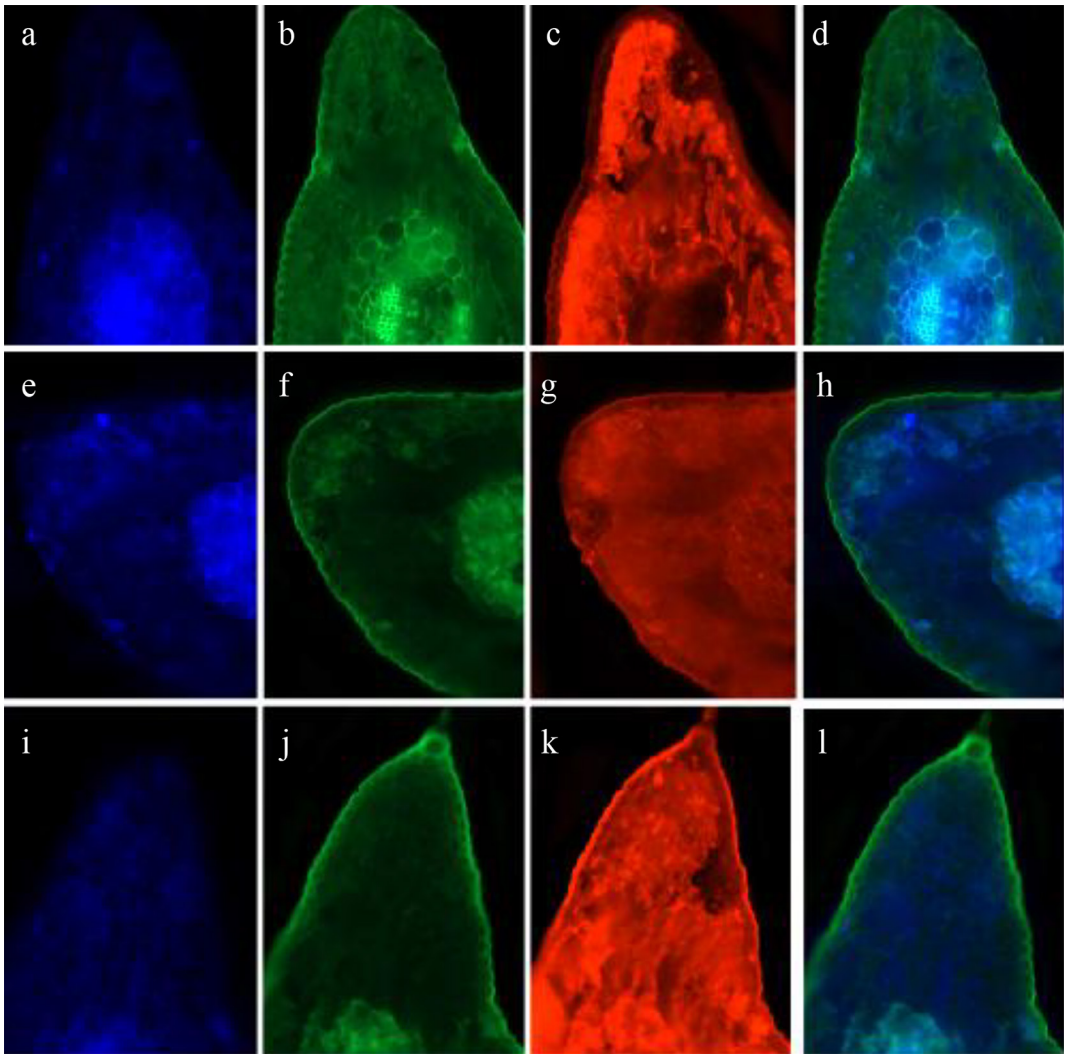

Figure 3. Autofluorescence of needle tissues in Scots pine seedlings: a–d – clone D1, e–h – clone D21, i–l – clone D22; filter channels: a, e, i – DAPI (λ_{exc} = 357/44 nm; λ_{em} = 447/60 nm); b, f, j – GFP (λ_{exc} = 482/25 nm; λ_{em} = 524/24 nm); c, g, k – Texas Red (λ_{exc} = 585/29 nm; λ_{em} = 628/32 nm); d, h, l – merged image

and phloem width were the most significant features distinguishing seedlings of different clones. Overall, of the 10 traits selected for comparison, only 2 did not show statistically significant differences among clones ($p < 0.05$) based on VIP (Variable Importance in Projection) scores for anatomical traits, as determined by the PLS-DA model for the first principal component. This plot shows the contribution of each anatomical trait to the formation of this component. The length of each arrow corresponds to the importance of the trait, while its direction indicates the nature of the relationship with the component. The color scale reflects VIP values characterizing the influence of each trait on class separation. Among the marker traits with high VIP scores, phloem width and epidermal cell width contributed most to clone discrimination, followed by resin duct sclerenchyma cell thickness and resin duct diameter. Thus, clear quantitative differentiation between productive and low-productivity clones was observed for the majority of the anatomical parameters examined.

Taken together, the multivariate analysis results enabled visualization of the overall data structure and identification of clone distribution patterns in the principal component space, while discriminant analysis complemented the comprehensive picture of differences in needle anatomy among Scots pine clones.

Overall, the biometric investigations revealed pronounced polymorphism among Scots pine seedlings in key morphometric parameters, indicating substantial interclonal variability already at

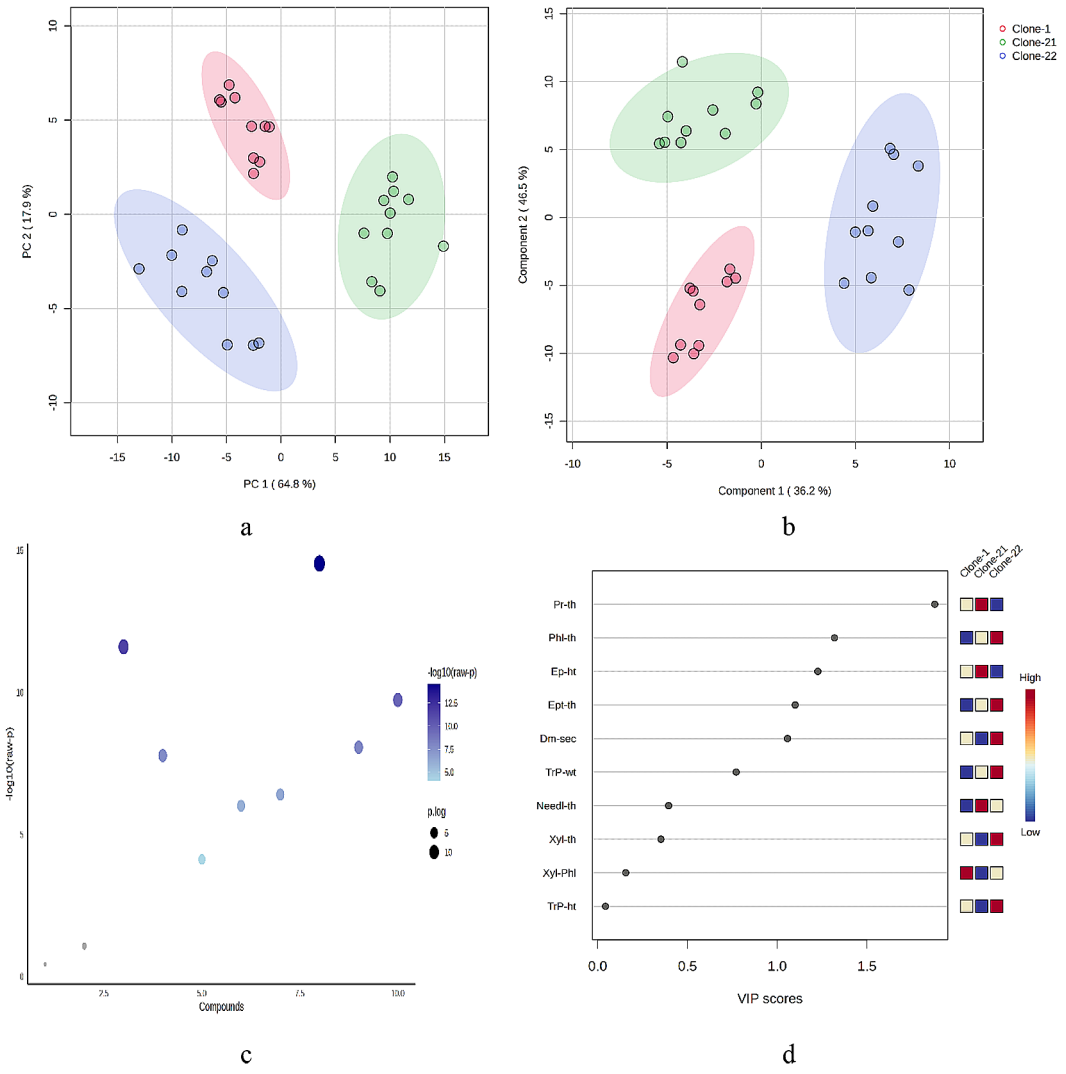

Figure 4. Results of multivariate analysis of Scots pine needle anatomical traits using principal component analysis (a) and partial least squares discriminant analysis (b); one-way ANOVA results for needle anatomical traits (c); VIP (variable importance in projection) score plot for needle anatomical traits based on the first principal component selected by the PLS-DA model (d). TrP-ht - endodermis cell width, TrP-wt – endodermis cell thickness, Pr-th – plicate mesophyll width, Ep-ht – epidermal cell width, Xyl-th – xylem width, Phl-th – phloem width, Xyl-Phl – xylem-to-phloem width ratio, Dm-sec – resin duct diameter, Ept-th – resin duct sclerenchyma cell thickness, Needl-th – vascular bundle radius

early ontogenetic stages. The statistically significant interclonal variability in morpho-anatomical needle traits observed in *Pinus sylvestris* L. seedlings indicates early differentiation of the assimilatory apparatus structures, driven by the genetic background of the clones. The results obtained are consistent with findings from previous studies indicating the high sensitivity of needle anatomy to genetic and environmental factors (Reich and Oleksyn, 2008).

Considerable variability in parameters such as cuticle thickness, hypodermis development, and plicate mesophyll width may reflect differences in the degree of protective and assimilatory specialization of the needles. In particular, well-developed dermal tissues and hypodermis are regarded as structural elements that enhance needle resilience to water deficit and temperature extremes by reducing transpiration losses and stabilizing the internal water regime of the plant (Savill, 1991). Similar patterns have been described for *P. sylvestri*s along climatic gradients and are interpreted as adaptive responses to environmental stress conditions (Reich and Oleksyn, 2008).

Variability in vascular tissue characteristics and resin duct diameter indicates interclonal differences in the formation of the transport and defense systems of the needles. According to the

literature, vascular bundle architecture is related to the efficiency of water and assimilate transport, whereas resin ducts perform a defensive function and play an important role in responses to biotic damage and abiotic stress (Hofmann et al., 2024).

Multivariate analysis (PCA and PLS-DA) confirmed the complex nature of interclonal differentiation and enabled identification of the anatomical traits contributing most to clone separation. The application of such approaches is appropriate for the integrated assessment of morpho-anatomical variability, as they account for interrelationships among individual parameters and reduce the influence of random variation in individual traits.

The results suggest that needle anatomical traits may serve as informative markers for preliminary screening of seedlings with favorable adaptive and growth characteristics – particularly fast-growing genotypes – at early ontogenetic stages, bypassing the need for prolonged field trials, which is especially relevant under current climate change.

CONCLUSIONS

This study provides the first quantitative evidence that the morpho-anatomical structure of *Pinus sylvestris* L. needles at early ontogenetic stages differs significantly among clonal variants. Among the traits analyzed – needle length, cuticle thickness, epidermal cell parameters, hypodermis development, plicate mesophyll width, vascular tissue characteristics, and resin duct diameter – several were identified that reliably distinguish clones with high and low productivity. Multivariate analyses highlighted the most informative markers of interclonal differentiation, including phloem width, epidermal cell width, and resin duct diameter, which have not previously been quantitatively characterized in seedlings at early developmental stages. These results indicate that needle morpho-anatomical traits have the potential to serve as early indicators of clone growth performance and adaptive capacity, enabling accelerated seedling selection. Nevertheless, further studies involving larger populations and field conditions are required to validate their practical applicability. Overall, the study's objective was achieved, and the work addresses an existing gap by providing reproducible quantitative indicators linking needle anatomical structure with growth and adaptability.

The relative stability of morphometric parameters within individual clonal variants indicates that the observed differences are predominantly genetically determined. Multivariate statistical analysis (PCA and PLS-DA) provided clear discrimination among the studied clones and enabled identification of the most informative anatomical traits driving interclonal differentiation.

REFERENCES

1. Allen, C., Breshears, D., and McDowell, N. (2015). On underestimation of global vulnerability to tree mortality and forest die-off from hotter drought in the Anthropocene. *Ecosphere*, *6*(8):129. http://dx.doi.org/10.1890/ES15-00203.1
2. Babyn, O., Pinchuk, A., Derii, A., Boyko, O., Likhanov, A. (2024a). Influence of urban environment factors on morphometric parameters and accumulation of secondary metabolites in *Cercis canadensis* L. and *Cercis siliquastrum* 'Alba'**.** *Ukrainian Journal of Forest and Wood Science***,** *15*(1), 8–24. https://doi.org/10.31548/forest/1.2024.08**.**
3. Babyn, O., Pinchuk, A., Derii, A., Boyko, O., Sovakov, O. (2024b). Determination of potential drought and frost resistance on the basis of studies with vegetative parts of plants of the genus *Cercis* **L.** *In IOP Conference Series: Earth and Environmental Science*, 1429, 012019. IOP Publishing. https://doi.org/10.1088/1755-1315/1429/1/012019
4. Boyko, H., Puzrina, N. (2021). Influence of growing conditions on changes in the species composition of mycobiota of scots pine seeds. *Ukrainian Journal of Forest and Wood Science*, *12*(2), 50–57. https://doi.org/10.31548/forest2021.02.005
5. Boyko, H., Puzrina, N., Bondar, A., Hryb, V. (2021). The influence of microbial agents and biological preparations based on them on the biometric indicators of *Pinus sylvestris* L. seedlings. *Scientific works of the Forestry Academy of Sciences of Ukraine*, (23), 68–78. https://doi.org/10.15421/412128
6. Bracalini, M., Florenzano, G., Panzavolta, T. (2024). Verbenone affects the behavior of insect predators and other saproxylic beetles differently: Trials using pheromone-baited bark beetle traps. *Insects*, *15*(4), article number 260. https://doi.org/10.3390/insects15040260
7. Derii, A., Pinchuk, A., Babyn, O., Sovakov, O., Likhanov, A. (2024). Variability of secondary metabolism and morphogenesis of Ligustrum vulgare L. under different growing conditions in an urban environment. *Folia Forestalia Polonica, 66*(4), 317–330. https://doi.org/10.2478/ffp-2024-0024
8. Evert, R.F. *Esau's Plant Anatomy: Meristems, Cells, and Tissues of the Plant Body*. 3rd ed. Hoboken: John Wiley & Sons, 2006.

9. Fuchylo, Ya.D., Ivaniuk, I.D., Makukh, Ya.P., Yukhnovskyi, V.Yu., Remeniuk, S.O., Kusik, V.M. (2021). Prospects for the use of Scots pine in agroforestry on agricultural lands of Polissya, Ukraine. *Bioenergy*, (2), 28–30. https://doi.org/10.47414/be.2.2021.244120
10. Hofmann, S., Schebeck, M., Kautz, M. (2024). Diurnal temperature fluctuations improve predictions of developmental rates in the spruce bark beetle *Ips typographus*. *Journal of Pest Science*. https://doi.org/10.1007/s10340-024-01758-1
11. Hordiienko, M.I., Huz, M.M., Debryniuk, Yu.M., Maurer, V.M. (2005). *Forest Plantations*. Lviv: Kamula.
12. Humeniuk, V.V. (2015). Natural regeneration of Scots pine (*Pinus sylvestris* L.) stands affected by surface fires in the Central Polissya region of Ukraine. *Scientific Bulletin of UNFU*, 25(5), 48–55. https://nv.nltu.edu.ua/index.php/journal/article/view/986
13. IPCC. (2021). *Climate Change 2021: The Physical Science Basis*. Contribution of Working Group I to the Sixth Assessment Report of the Intergovernmental Panel on Climate Change. Cambridge University Press. https://doi.org/10.1017/9781009157896
14. Lovynska, V., Terentiev, A., Lakyda, P., Sytnyk, S., Bala, O., Gritsan, Y. (2021). Comparison of Scots pine growth dynamics in Polissya and Steppe zone of Ukraine. *Journal of Forest Science*, *67*(11), 533–543. https://doi.org/10.17221/93/2021-JFS
15. Oberhuber, W., Hammerle, A., Kofler, W. (2015) Tree water status and growth of saplings and mature Norway spruce (*Picea abies*) at a dry distribution limit. *Front. Plant Sci. 6*, 703. https://doi.org/10.3389/fpls.2015.00703
16. Reich, P., Oleksyn, J. (2008). Climate warming will reduce growth and survival of Scots pine except in the far north. *Ecology Letters*, *11*, 588–597. https://doi.org/10.1111/j.1461-0248.2008.01172.x
17. Pinchuk, A., Ivanyuk, I., Shevchuk, M., Dubchak, M., Likhanov, A. (2021). Effect of rutin-ammonium complex on the physiological state of Scots pine seedlings. *Ukrainian Journal of Forest and Wood Science*, 12(4), 83–91. https://doi.org/10.31548/forest2021.04.008
18. Pinchuk, A., Likhanov, A., Ivanyuk, I., Spivak, M. Ya. (2020). Influence of ceo2 nanoparticles on seed germination and synthesis of phenols in spruce seedlings. *Ukrainian Journal of Forest and Wood Science*, *11*(3), 36–44. https://doi.org/10.31548/forest2020.03.004
19. Tereshchenko L. I., Gordiyashchenko, A. Y., Samoday, V. (2020). Variability and relationships of morphological and anatomical characteristics of Scots pine needles in the fresh relatively infertile pine site. *Forestry and Forest Melioration*, (137), 32–40. https://doi.org/10.33220/1026-3365.137.2020.32
20. Savill, P. S. (1991). *The silviculture of trees used in British forestry*. CAB International.
21. Vaganov, E.A., Hughes, M.K., Shashkin, A.V. (2006). *Growth Dynamics of Conifer Tree Rings: Images of Past and Future Environments*. Berlin: Springer.